N. Lebedev, I. I. Farbstein, S. S. Shalyt, E. S. Itskevich, and V. A. Sukhopavov, International Colloquium GNRS, Report No. 188, Grenoble, 1970, p. 143 (unpublished).

[21]V. B. Anzin, M. S. Bresler, I. I. Farbstein, E. S. Itskevich, Yu V. Kosichkin, V. A. Sukhopavov, A. S. Telepnev, and V. G. Veselago, Phys. Status Solidi b48, 531 (1971).

[22]E. Bangert and W. Dreybrodt, Solid State Commun. 10, 623 (1972).

[23]R. Kubo, J. Phys. Soc. Japan 12, 570 (1957).

[24]J. R. Apel, T. O. Poehler, C. R. Westgate, and R. I. Joseph, Phys. Rev. B 4, 2 (1971).

[25]A. Kawabata, J. Phys. Soc. Japan 23, 999 (1967).

[26]M. Selders and P. Grosse (private communication).

PHYSICAL REVIEW B VOLUME 6, NUMBER 6 15 SEPTEMBER 1972

Optical Properties of K between 4 and 10.7 eV and Comparison with Na, Rb, and Cs†

U. S. Whang* and E. T. Arakawa

Health Physics Division, Oak Ridge National Laboratory, Oak Ridge, Tennessee 37830

and

T. A. Callcott‡

Department of Physics, The University of Tennessee, Knoxville, Tennessee 37916

(Received 13 March 1972)

The optical and dielectric constants of K have been determined from reflectance and transmission measurements for photons of energy between 4.0 and 10.7 eV. Reflectance measurements were made as a function of incident angle at a K-MgF_2 interface in an ultrahigh-vacuum system. The refractive index (n) was determined from the critical angle for total internal reflection and the absorption coefficient (k) from the slope of the reflectance curve at the critical angle and from transmission measurements. The real part of the dielectric function (ϵ_1) and the optical conductivity $\sigma = \omega\epsilon_2/4\pi$ were derived from n and k. In σ we find a broad peak centered at 8 eV. This absorption peak is discussed along with comparable peaks in Na, Rb, and Cs. One-electron and many-body processes that might give absorption in this energy region are discussed. ϵ_1 is analyzed in terms of a nearly-free-electron model to obtain a value of the effective mass (m_{eff}) and of the contribution of core polarization ($4\pi n_0\alpha$) to ϵ_1. We find $4\pi n_0\alpha = 0.15 \pm 0.01$ and $m_{eff}/m_0 = 1.01 \pm 0.01$.

INTRODUCTION

This is the last of a series of papers[1-3] by the present authors reporting measurements of the optical properties of the alkali metals Cs, Rb, and K for photons of energy between 3.5 and 11 eV. Similar measurements have been reported by Sutherland and Arakawa[4] for Na. Optical measurements on these metals at energies below the plasma frequency give results in fair agreement with a nearly-free-electron (NFE) model that includes the effects of free-carrier absorption and interband transitions between the filled conduction band and the next-higher band.[5-7]

Our measurements clearly show the existence of an additional absorption process in all of the alkalies at energies above the plasma frequency. In previous papers, broad strong absorption peaks in the optical conductivity have been reported in Cs and Rb with maxima at 5 and 6.8 eV, respectively. A weaker peak is centered at 10 or 11 eV in Na.

This paper is divided into two parts. In the first part, we report experimental determinations of the index of refraction (n), the absorption coefficient (k), the real and imaginary parts of the dielectric response function (ϵ_1 and ϵ_2), and the optical conductivity (σ) of K for photon energies of 3.3 to 10.7 eV. In σ, we find a broad absorption peak centered at 8 eV that is similar to the peaks observed in the other alkalies. A Kramers-Kronig analysis applied to $\epsilon_2 = 4\pi\sigma/\omega$ is used to calculate the effect of interband transitions and of the broad high-energy peak on ϵ_1. When these contributions are subtracted, the remaining portion of ϵ_1 represents that expected for a NFE model containing only free-carrier absorption. These corrected values of ϵ_1 are used to obtain values of the effective mass and of the core polarization, which are the adjustable parameters of such a free-electron model.

In the second part of the paper, we briefly summarize the optical properties of all of the alkali metals between Na and Cs for photon energies above their plasma frequencies. Plots are given of σ for these four materials. The broad absorption peaks in σ are found to become stronger and move to lower energies for alkali metals of larger atomic num-

ber. Several processes that may account for this absorption are discussed. Also, the values of core polarization and effective mass obtained from our analysis of ϵ_1 in terms of the NFE model are tabulated for K, Rb, and Cs.

EXPERIMENTAL PROCEDURES

The basic experimental procedures used in this work have been described in detail in earlier papers.[2,3] The sample chamber is shown schematically in Fig. 1. Optical constants were obtained from measurements of the reflectance as a function of the angle of incidence $[R(\theta)]$ and from transmission measurements.

In the reflectance measurements, K was deposited on the flat surface of a MgF_2 semicylinder substrate. Light is incident on the K film through this substrate. A semicylinder is used so that incident and reflected beams pass through the vacuum-substrate interface at normal incidence for all reflection angles. The sample holder and light-pipe detector are connected through a gear mechanism which rotates the light-pipe detector through twice the angle of the sample and thus keeps the face of light pipe in the reflected beam throughout the experiment. $R(\theta)$ curves were taken between angles of 5° and 84°. At angles less than 5° the incident beam was blocked by the light pipe and at angles greater than 84° by the mounting structure of the semicylinder.

K was deposited on only one-half of the substrate surface. The remaining half was used as a reference surface having a substrate-vacuum interface. $R(\theta)$ curves made at this vacuum interface gave values of the total incident-beam intensity and of the index of refraction of the substrate which were used in the analysis of $R(\theta)$ data from K. The analysis of $R(\theta)$ also requires knowledge of the polarization of the incident light. This was measured using a gold-coated triple-reflection polarizer.[8]

For the transmission measurements, K was deposited on MgF_2 substrates of uniform thickness. The transmittance provides a straightforward and accurate measurement of the absorption coefficient (k) if the thickness of the absorber is known. Since we had no independent means of measuring film thickness accurately, only relative values of k as a function of photon energy were obtained from these measurements. These values of k were normalized to absolute values obtained from measurements of $R(\theta)$. Film thicknesses indicated by this normalization were very reasonable.

Procedures for cleaning substrates and making evaporations were the same as those previously described[3] for Rb. In brief, K was evaporated from 0.5-g ampoules of 99.8% K onto slightly cooled substrates. Pressures in the chamber were about 5×10^{-10} Torr before evaporation as measured by a nude ion gauge. Pressures during the 3-min evaporations were in the 10^{-7} Torr range and returned to about 2×10^{-9} Torr after the evaporation was com-

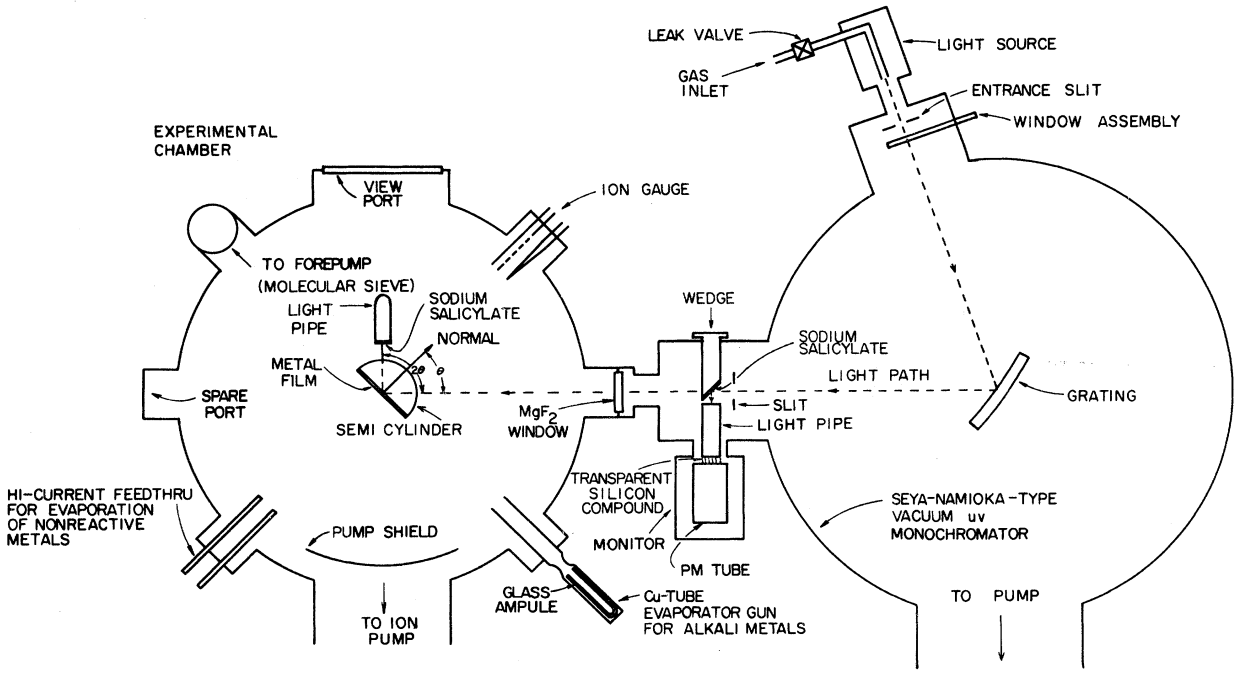

FIG. 1. Schematic diagram of apparatus.

plete. Thereafter the pressure increased slowly with time to about 10^{-8} Torr. This relatively high pressure results from the high vapor pressure of K, so that most of the residual gas consisted of K molecules, with much smaller partial pressures of other gases. Both the vacuum and substrate surfaces of the films were specular to the eye after evaporation. Reflectance measurements made through the substrate were unchanged after many hours. Significant changes in the transmittance were measurable after 2–3 h. The transmission measurements reported here were made within about 1 h after the evaporation was complete.

Determination of n and k

In general, $R(\theta)$ depends upon n, k, and the polarization of the light. If the polarization is known, $R(\theta)$ may be fitted to Fresnel's equations to obtain n and k. A specialized variation of this general method was used in our analysis of $R(\theta)$ to obtain n and k. A chief virtue of our method is that it concentrates on two features of the $R(\theta)$ curves that depend strongly on n and k, respectively, with little dependence on the other variables.

Above the plasma frequency, the alkali metals are nearly transparent. For K, at photon energies above about 4 eV, $n \simeq 1$ and $k < 0.1$. Since light is incident on a K film through a substrate of higher index of refraction, there is a critical angle for total internal reflection given by Snell's law. If k were zero, Snell's law would be

$$n_{\mathrm{rel}} = n/n_s = \sin\theta_c , \tag{1}$$

where n_s is the index refraction of the substrate and θ_c is the critical angle. There is a discontinuity in the slope of $R(\theta)$ at θ_c as shown in Fig. 2. If $0 < k \lesssim 0.1$, the discontinuity is removed, but there is an inflection point in the $R(\theta)$ curve that lies close to the critical angle for zero absorption. Like θ_c, this angle of maximum slope (θ_m) is strongly dependent on n and only weakly dependent on k and the polarization. We will refer to θ_m as the critical angle for finite k. Using calculated curves published by Hunter, it is possible to make small corrections for k and the polarization in the range $k < 0.2$, so that n may be obtained from θ_m and an approximate value of the other two variables.[9]

We have shown in earlier papers that the slope of the $R(\theta)$ curve at θ_m depends strongly on k_{rel} ($= k/n_s$) but very weakly on n_{rel} and the polarization.[2,3] The strong dependence on k is clear in Fig. 2. In particular, for $0.2 \leq n_{\mathrm{rel}} < 1$ and $0.02 \leq k_{\mathrm{rel}} \leq 0.12$, the slope of $R(\theta)$ at θ_m determines the value of k_{rel} within 5% for all polarizations and values of n_{rel} in this range. The explicit dependence of k_{rel} on slope for a large range of n_{rel} and polarizations will be discussed in a separate paper.[10] Using these curves and Hunter's calculations, one can determine n and k from the angular position of θ_m and the magnitude of the slope of $R(\theta)$ at this angle without reference to the remaining portions of the $R(\theta)$ curves.

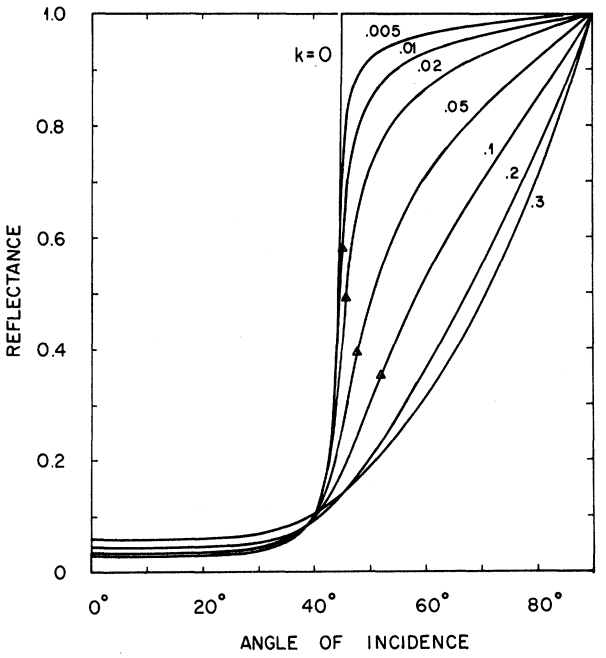

FIG. 2. Calculated reflectance as a function of incident angle for $n_{\mathrm{rel}} = 0.7$ ($\theta_c = 44°\ 26'$) and different values of k_{rel}. Triangles are the positions of θ_m's. The values are 44° 30′ for both $k_{\mathrm{rel}} = 0.005$ and 0.01; 45° 0′ for $k_{\mathrm{rel}} = 0.02$; 45° 54′ for $k_{\mathrm{rel}} = 0.05$; and 49° 26′ for $k_{\mathrm{rel}} = 0.1$. The $R(\theta)$ curves for $k_{\mathrm{rel}} = 0.2$ and 0.3 have no inflection point, and thus the critical angle cannot be determined for these curves.

In practice, the limitation on the accuracy of the values of k obtained from the slope at θ_m is determined by the accuracy with which the reflectance curve can be normalized to the incident-beam intensity. This normalization problem limits the accuracy of the determination of slope and hence the accuracy of k, but does not significantly affect the determination of θ_m and n.

We have found that the values of n and k determined from θ_m and the slope at θ_m are more reproducible from sample to sample and substrate to substrate than are values determined by fitting $R(\theta)$ over the full range of experimental angles.[3] This essentially results from the fact that $R(\theta)$ near θ_m is less subject to distortion by experimental problems such as scattered light and interface contamination.

Values of n and k obtained from reflectance measurements are shown in Fig. 3 as open circles and triangles, respectively. Values of k obtained from transmission measurements are shown as

solid circles. The transmission data were normalized to the reflectance data in the region near 1500 Å. The values of n show scatter of about 2% about the smooth plotted curve. Values of k have a scatter of about 6% about the smooth curve above 1300 Å. In the region below 1300 Å, transmission measurements provide the most accurate data for k since values of k_{rel} are small ($\lesssim 0.02$) and difficult to determine from $R(\theta)$. The transmission data show a scatter of about 3% in this region.

Values of n and k taken from the smoothed curves of Fig. 3 were used in all subsequent analyses. Table I gives the values of n, k, ϵ_1, ϵ_2, and σ obtained from these smoothed curves.

Analysis of Data for K

Figure 4 is a plot of the optical conductivity of K derived from the smoothed n and k values using the relation $\sigma = nk\omega/2\pi$. σ is a measure of the rate of energy absorption by the solid. Data obtained by other workers at lower energies are also plotted.[4,6,11–13] Smith's data, obtained from ellipsometry measurements, most clearly show the absorption peak centered at 2 eV that may be attributed to direct interband transitions and the rise in σ below 1 eV due to free-carrier absorption. The dominant feature of the σ curve in the region of our measurements is a broad strong peak centered at 8 eV and extending from about 5 to 11 eV. Its interpretation will be discussed in a later section of this paper.

Figure 5 is a plot of ϵ_1 vs the wavelength squared. The solid triangles are points calculated from the smoothed values of n and k using the relation $\epsilon_1 = n^2 - k^2$. Except for the open circles the other points plotted are taken from the data of other workers. Their data are in generally good agreement with ours except at the shortest wavelengths.

We will compare the data for ϵ_1 with the equation derived by Cohen on the basis of a NFE model.[7] It may be written

$$\epsilon_1 = 1 + 4\pi n_0 \alpha - \omega_a^2/\omega^2 + \delta\epsilon_1(\omega) , \tag{2}$$

where

$$\omega_a^2 = 4\pi n_0 e^2/m_{eff} , \tag{3}$$

n_0 is the number of ions or conduction electrons per unit volume, $4\pi n_0\alpha$ is the contribution of the core electrons to the polarization, m_{eff} is the average effective mass of the conduction-band electrons, ω_a is the plasma frequency when only free-carrier absorption is included, and $\delta\epsilon_1(\omega)$ is the contribution to ϵ_1 of all absorption processes affecting the conduction-band electrons except free-carrier absorption. It should be noted that m_{eff} is the true effective mass and not the so-called "optical" effective mass obtained by fitting to ϵ_1 an equation similar to (2) but without the final $\delta\epsilon_1$ term.

$\delta\epsilon_1(\omega)$ may be calculated using the Kramers-Kronig relation in the form

$$\delta\epsilon_1 = 8\int_0^\infty \delta\sigma(\omega')/(\omega'^2 - \omega^2)\,d\omega' , \tag{4}$$

when $\delta\sigma(\omega')$, the contribution to σ of all absorption processes except free-carrier absorption, is known. In the $\sigma(\omega)$ plot, the free-carrier absorption at energies below 1 eV may be fitted by a Drude absorption term

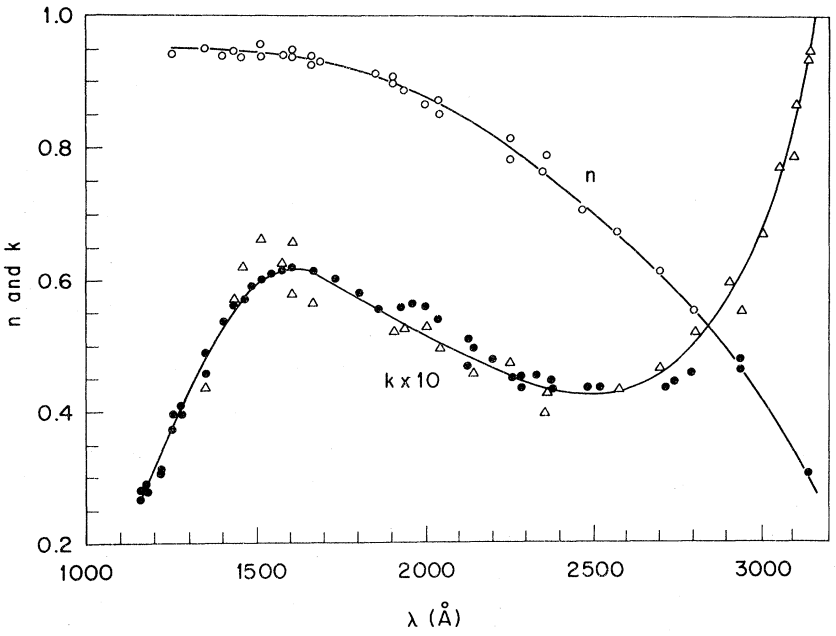

FIG. 3. Experimental values of n and k for K films on the MgF_2 substrate. Open circles are n values obtained from the critical-angle method, triangles are k values obtained from slope of $R(\theta)$ near critical angle, and solid circles are k values obtained from transmission measurements. Solid lines give the smoothed average values of the data.

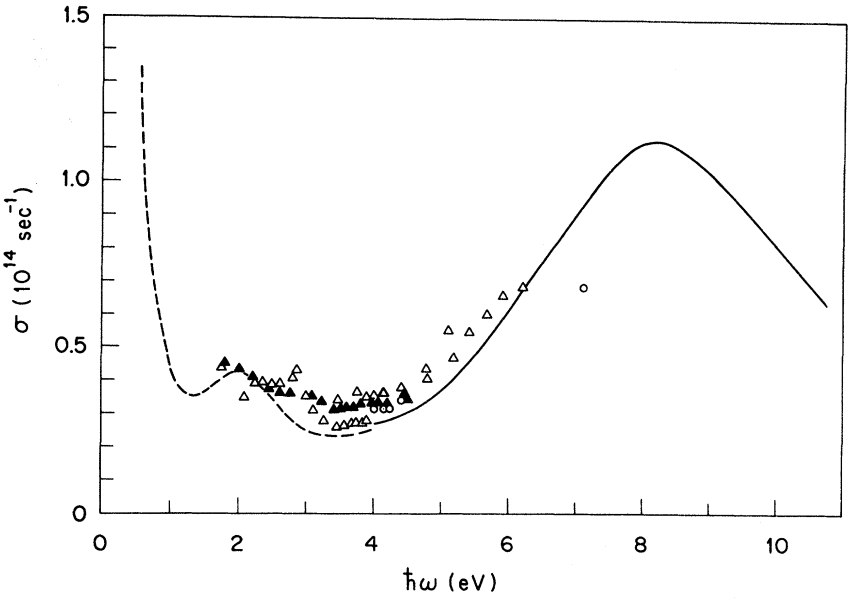

FIG. 4. Optical conductivity of K vs photon energy. The solid line is obtained from the averaged smooth curve of n and k in Fig. 3. Dashed line is from data of Smith (Ref. 6). Data points are taken from Sutherland *et al.* (Ref. 4) (○), Yamaguchi and Hanyu (Ref. 11) (△), Palmer and Schnatterly (Ref. 12) (▲).

$$\sigma_D = \tfrac{1}{2}\gamma\{\omega_a^2/[\omega^2+(2\pi\gamma)^2]\}\,, \qquad (5)$$

characterized by a damping constant of $2\pi\gamma\hbar = 0.018$ eV and a plasma energy of 3.9 eV. When this is subtracted from the total conductivity and the remaining $\delta\sigma$ is used in Eq. (4), we obtain the values of $\delta\epsilon_1(\omega)$ shown in Fig. 6. For this calculation $\delta\sigma$ was separated rather roughly into two parts representing the interband peak and the high-energy peak. The contributions of each part to ϵ_1 are shown as $\delta\epsilon_1(I)$ and $\delta\epsilon_1(P)$, respectively. The total $\delta\epsilon_1$ shown as a solid line is independent of the details of this separation. In performing the integral in Eq. (4) $\delta\sigma$ was extrapolated smoothly to zero at energies above our experimental data.

The open circles in Fig. 5 show the values of $\epsilon_1 - \delta\epsilon_1$ obtained when the contributions of the high-energy absorption processes are subtracted from ϵ_1. The straight line shows the best fit of Eq. (2) to these data. Table II gives values of m_{eff} and $4\pi n_0\alpha$ obtained from this fit as well as the plasma energy $\hbar\omega_p$ obtained by setting $\epsilon_1 = 0$. The table also includes values of these parameters obtained from a variety of experiments by other workers.[4,6,11–19] The values of m_{eff} and $\hbar\omega_a$ obtained from measurements in the visible and infrared are not directly comparable with our values since in most cases no corrections were made for the effect of $\delta\epsilon_1$. Smith made the corrections but did not, of course, include the effect of the high-energy absorption peak. If our corrections were applied to his data, values of $\hbar\omega_a$ would be slightly smaller and values of m_{eff} slightly larger than those shown in the table.

As was noted in the earlier report on Rb, the effective masses that give the best fit to our data in the vacuum ultraviolet are consistently smaller than those providing the best fit to the data at lower energies. This result cannot be understood within the framework of Cohen's theory. Because our data extend to higher energies, and because of our

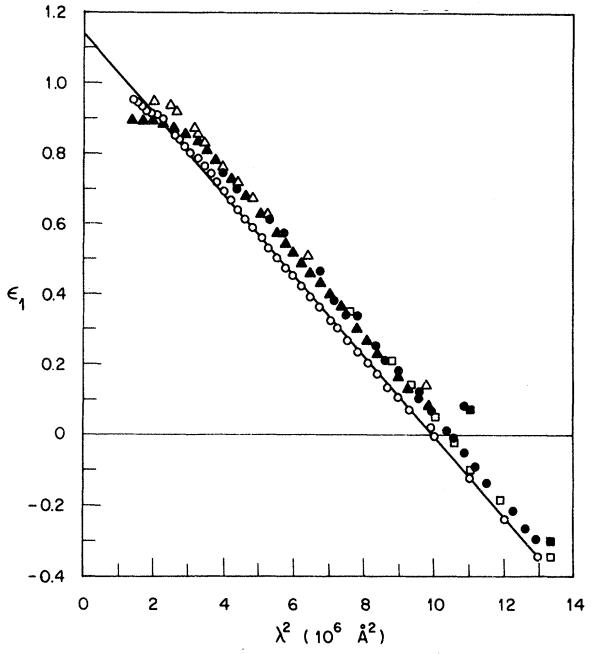

FIG. 5. Real part of the complex dielectric constant of K vs square of photon wavelength. Solid triangles are the points obtained from the smooth curve of n and k values. Data points are taken from Sutherland *et al.* (Ref. 4) (△), Yamaguchi and Hanyu (Ref. 11) (●), Palmer and Schnatterly (Ref. 12) (□), and Smith (Ref. 6) (■). Open circles are a plot of $\epsilon_1 - \delta\epsilon_1$, the free-carrier contribution to ϵ_1.

careful subtraction of the effects of high-energy absorption processes, we believe that our values of the core polarization are the best so far obtained.

SUMMARY OF RESULTS FOR K, Rb, Cs

A summary of the values of m_{eff}, $4\pi n_0\alpha$, $\hbar\omega_a$, and $\hbar\omega_p$ obtained by fitting Eq. (2) to ϵ_1 data from K, Rb, and Cs is given in Table III. In each case, the effects of high-energy absorption processes were subtracted using conductivity data and Eq. (4) as described above for K. The reader is referred to the papers on Rb [2] and Cs [3] for plots of $\epsilon_1(\omega)$, the details of the analysis of data from these materials, and for a comparison of our values to those obtained by other workers.[2,3] In all of the materials, it is observed that the effective masses obtained by fitting data in the ultraviolet to Eq. (2) are smaller than effective masses obtained by fitting infrared data. The source of this difference is not understood.

The optical conductivities of the four alkalies from Na to Cs are plotted in Fig. 7. For K, Rb, and Cs, the solid lines at high energies are from the work of the present authors. The two solid lines for Na are from data taken from two different samples by Sutherland.[4] The dashed curves at low energies are from the work of Smith.[6] The dash-dot curve for Na is a smooth extrapolation between the high- and low-energy data. The primary features of interest in the plots of conductivity in Fig. 7 are the high-energy peaks which occur above the plasma frequency in each of these materials.

We have performed optical-sum-rule calculations using the data summarized in Fig. 7 and the expression

$$n_{eff}=\frac{2}{\pi}\frac{m_0}{e^2}\frac{1}{n_0}\int_0^{\omega}\sigma(\omega')\,d\omega', \qquad (6)$$

where n_0 is the number of atoms per unit volume and m_0 is the free-electron mass. n_{eff} is a measure of the oscillator strength associated with optical-transition matrix elements at frequencies below ω, and can be thought of as the number of electrons per atom involved in optical-absorption processes

TABLE I. Optical and dielectric constants of K.

λ (Å)	$\hbar\omega$ (eV)	n	k	ϵ_1	ϵ_2	σ (10^{14} sec^{-1})
1160	10.69	0.945	0.027	0.892	0.050	0.648
1200	10.33	0.945	0.031	0.892	0.059	0.732
1250	9.92	0.945	0.037	0.892	0.070	0.839
1300	9.54	0.945	0.042	0.891	0.079	0.916
1350	9.13	0.945	0.048	0.891	0.090	0.998
1400	8.86	0.945	0.052	0.890	0.098	1.05
1450	8.55	0.943	0.056	0.886	0.110	1.09
1500	8.27	0.941	0.060	0.882	0.110	1.12
1550	8.20	0.939	0.061	0.878	0.120	1.12
1600	7.98	0.935	0.062	0.870	0.110	1.09
1650	7.52	0.931	0.061	0.863	0.110	1.04
1700	7.29	0.926	0.060	0.854	0.110	0.980
1750	7.09	0.921	0.059	0.845	0.110	0.932
1800	6.89	0.915	0.057	0.834	0.110	0.876
1850	6.70	0.906	0.056	0.818	0.100	0.823
1900	6.53	0.895	0.055	0.798	0.098	0.771
1950	6.36	0.883	0.053	0.777	0.094	0.720
2000	6.20	0.870	0.052	0.754	0.090	0.672
2050	6.05	0.855	0.050	0.729	0.086	0.626
2100	5.91	0.842	0.049	0.707	0.082	0.587
2150	5.77	0.826	0.048	0.680	0.079	0.548
2200	5.64	0.810	0.046	0.654	0.075	0.512
2250	5.51	0.794	0.045	0.628	0.072	0.479
2300	5.39	0.776	0.044	0.600	0.069	0.447
2350	5.28	0.758	0.044	0.573	0.066	0.421
2400	5.17	0.740	0.043	0.546	0.064	0.398
2450	5.06	0.720	0.043	0.517	0.061	0.376
2500	4.96	0.70	0.043	0.488	0.060	0.357
2550	4.86	0.68	0.043	0.461	0.058	0.342
2600	4.77	0.66	0.043	0.434	0.057	0.330
2650	4.68	0.637	0.044	0.401	0.056	0.319
2700	4.59	0.610	0.046	0.370	0.056	0.310
2750	4.51	0.580	0.048	0.334	0.055	0.302
2800	4.43	0.550	0.050	0.300	0.055	0.296
2850	4.35	0.520	0.053	0.268	0.055	0.291
2900	4.28	0.485	0.057	0.232	0.055	0.285
2950	4.20	0.450	0.061	0.199	0.055	0.279
3000	4.13	0.412	0.067	0.165	0.055	0.274
3050	4.07	0.375	0.073	0.135	0.055	0.270
3100	4.00	0.335	0.082	0.106	0.055	0.266
3150	3.94	0.303	0.095	0.083	0.058	0.274

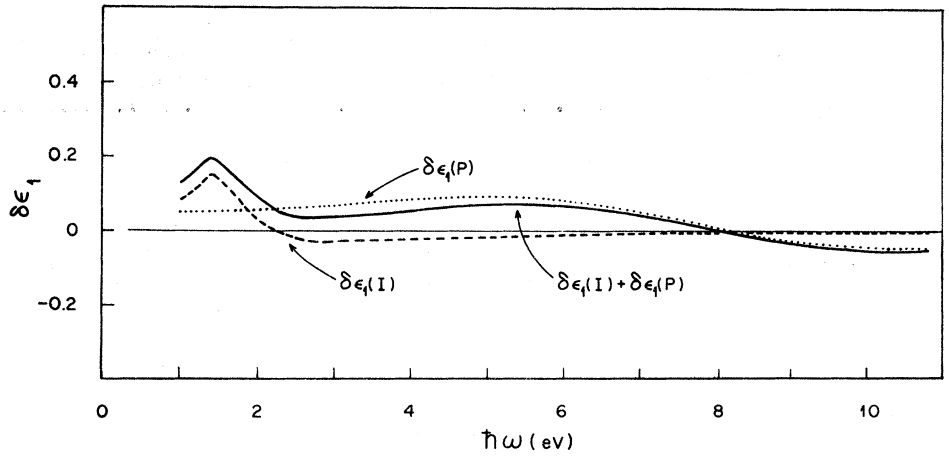

FIG. 6. $\delta\epsilon_1$ vs photon energy of K. $\delta\epsilon_1$ (*I*) and $\delta\epsilon_1$ (*P*) represent the contributions to ϵ_1 of the interband transitions and plasmon-assisted transitions, respectively. Separate contributions to ϵ_1 add algebraically to give the solid line.

TABLE II. NFE parameters of K from optical data.

	$4\pi n_0\alpha$	$\frac{m_{eff}}{m}$	$\hbar\omega_a$ (eV)	$\hbar\omega_p$ (eV)
Vacuum ultraviolet				
Present	0.15	1.01	3.97	3.85
Yamaguchi and Hanyu	0.23	1.01		3.82
Sutherland and Arakawa	0.20			3.72
Visible and infrared				
Yamaguchi and Hanyu	0.14	1.03		
Smith		1.06		3.8
Palmer and Schnatterly		1.08		
Ives and Briggs (Cohen's analysis)	0.29	1.08		3.67
Mayer and El Naby	0.11	1.00		4.25
Near and far infrared				
Althoff *et al.*		1.17		
Hodgson		1.18		
Energy loss				
Kunz				3.72
Robin and Best				3.87
Swan				4.05
Yamaguchi and Hanyu (from optical data)				3.83

for photon energies below $\hbar\omega$. For the alkali metals, n_{eff} is expected to approach approximately 1 as the oscillator strength for transitions of the valence electrons is exhausted.[20] For metals with free-carrier absorption, such calculations are complicated by the necessity of extrapolating $\sigma(\omega)$ to zero frequency. We have assumed that for photon energies below $E_0=\hbar\omega_0=0.5$ eV $\sigma(\omega)$ may be represented by a Drude term of the form of Eq. (5). Below this energy, Eq. (6) may be integrated explicitly so that

$$n_{eff}=\frac{2}{\pi}\frac{m_0}{m_{eff}}\tan^{-1}\frac{E_0}{2\pi\gamma\hbar}+\frac{2}{\pi}\frac{m_0}{\hbar e^2}\frac{1}{n_0}\int_{E_0}^{E}\sigma(E')dE'. \tag{7}$$

$2\pi\gamma\hbar$ may be estimated from dc conductivity measurements or from infrared optical data.[6] For Na, K, Rb, and Cs such estimates range from a low value of about 0.015 eV for K up to about 0.030 eV for Cs. For this range of values and $E_0=0.5$ eV, $(2/\pi)\tan^{-1}(E_0/2\pi\gamma\hbar)$ has values ranging from 0.98 for K to 0.96 for Cs. Consequently, the mass ratio m_0/m_{eff} chiefly determines the value of the first term.

There is much uncertainty as to what effective-mass values should be used. It certainly seems appropriate to use the relatively large effective masses derived from fitting infrared optical data rather than those obtained by fitting optical data at photon energies above 4.0 eV. Even with this restriction, a large range of values of m_{eff} has been reported. Effective masses derived from the infrared measurements of other workers are summarized in Table II for K, in our previous papers for Rb and Cs, and in Ref. 4 for Na. Using these values of m_{eff}, the first term of Eq. (7) is found to have a range of values between 0.76 and 0.90 for Na, 0.83 and 0.90 for K, 0.76 and 0.84 for Rb, and 0.66 and 0.80 for Cs.

The contribution to n_{eff} of the second term in Eq. (7) for each of the alkalies is plotted in Fig. 8. The plots are obtained from a numerical integration of the conductivity values plotted in Fig. 7.

Adding the contribution from the Drude term and the values plotted in Fig. 8, the total value of n_{eff} up to photon energies of about 10 eV is found to be smaller than 1 for Na and to increase with atomic number. It is approximately equal to 1 for K, slightly larger than 1 for Rb, and considerably greater than 1 for Cs.

Several factors may cause the optical sum rule to give values greater than 1 for the heavier alkali metals. Chief among these is the fact that the sum rule is exact only when it applies to all electrons in the atom and the integral in Eq. (6) is taken over all frequencies. The expression should sum to 1 for the transitions of the conduction electrons alone only in the approximation that the interaction of the conduction-band states with the core states can be neglected. In Rb and Cs, the core levels are known to be relatively close to the conduction-band states (~12 eV for Cs, ~15 eV for Rb) and to interact strongly with conduction-band states.[21] This will tend to increase the value of n_{eff} above 1 for these materials. A second factor that may contribute is that the simple extrapolation of $\sigma(\omega)$ to zero using a Drude term may be substantially in error. In addition to the uncertainties in the effective masses used, there may be substantial deviations from the Drude form, particularly in the case of the heavier alkali metals which deviate rather strongly from free-electron behavior.

If the experimental values of $\sigma(\omega)$ for Cs are substantially in error, it seems much more likely that the experimentally determined interband or high-energy peaks are too large, rather than that they are absent. In the case of Cs, which has the largest value of n_{eff}, Mayer and Hietel found a considerably smaller interband peak than did Smith.[4,6] For our data on Cs, the magnitude of the high-energy peak is rather uncertain (~30%) due to an uncertainty in the scaling factor related to the normal-

TABLE III. NFE parameters of K, Rb, and Cs.

	$4\pi n_0\alpha$	$\frac{m_{eff}}{m_0}$	$\hbar\omega_a$ (eV)	$\hbar\omega_p$ (eV)
K	0.15±0.01	1.01±0.01	3.97±0.01	3.85
Rb [a]	0.25±0.02	1.03±0.02	3.40±0.03	3.33
Cs [b]	0.37±0.01	1.05±0.05	2.87±0.07	...

[a]From Ref. 3. [b]From Ref. 2.

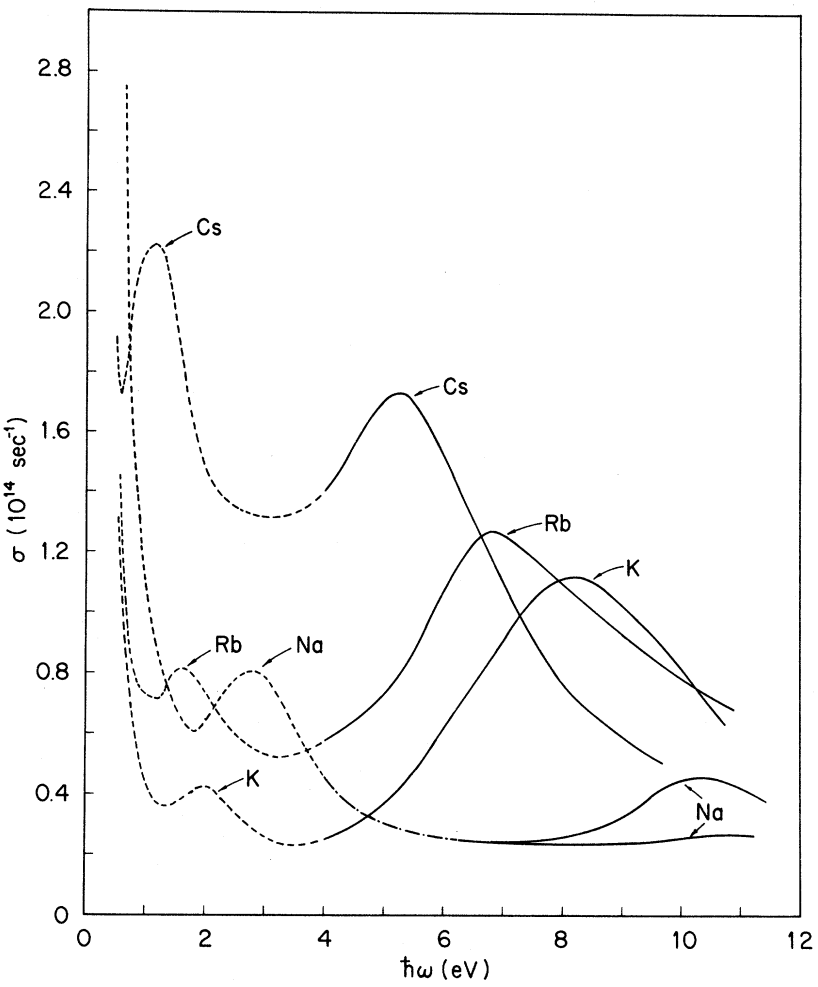

FIG. 7. Optical conductivity vs photon energy of Na, K, Rb, and Cs. Solid lines for K, Rb, and Cs are from the present data, and the two solid lines for Na are from Sutherland's data with different films. The dash-dotted line is calculated from n and k values obtained by a smooth interpolation between Smith's and Sutherland's data.

ization of the $R(\theta)$ curves. This normalization factor renders the magnitude of $\sigma(\omega)$ uncertain by an approximately constant factor over the full range of our data, but does not significantly effect the peak position. The uncertainty in normalizing the $R(\theta)$ curves was much smaller in the case of Rb and K than for Cs.

The following characteristics of the peaks in σ seem to us to be important:

(i) They represent a strong energy-absorption process, comparable in magnitude to the interband absorption process.

(ii) In absolute magnitude, the data show some regularities in that the peaks occur at lower energies and are progressively stronger for materials of higher atomic number.

(iii) The relative magnitudes of the high-energy peak and the interband peak show no obvious regularities. In σ, their ratios are approximately 0.5, 2.5, 1.5, and 0.7 for Na through Cs.

(iv) In each material the high-energy peak is found about $1.5\hbar\omega_p$ above the interband peak, where $\hbar\omega_p$ is the plasma frequency. In Fig. 7, the separations are approximately 8, 6, 5, and 4 eV for Na through Cs. Values of $1.5\hbar\omega_p$ for these materials are 8.4, 6.0, 5.1, and 4.3 eV, respectively.

The question of interest is whether this absorption can be understood in terms of one-electron theory or whether it must be explained in terms of the excitation of collective modes of the solid.

In one-electron theory direct interband transitions from the conduction band to higher bands can contribute to absorption in this energy range for all of these metals. Energy-band calculations extending to energies about 10 eV above the Fermi level have been made by Kenney for Na, Rb, and Cs.[22] Ham's calculations are less extensive but include results for K.[23] In Na and K, mixed bands of predominant p and d character are spread over the region 5–10 eV above the conduction band. In Rb, mixed p and d states occupy the region from 2 to 4 eV above the conduction band, and f bands become important above 5 eV. In Cs, mixed p-d bands are found at 2–4 eV and a prominent set of f bands at 5–8 eV above the conduction-band states. Thus, in Na, K, and Rb transitions to fairly prominent bands of d

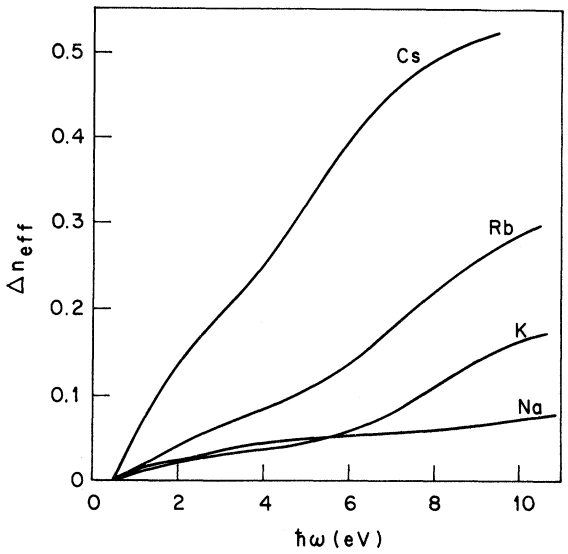

FIG. 8. Contribution to optical sum rule calculated from experimentally determined conductivities at photon energies above 0.5 eV.

and f states may contribute to absorption at 10, 8, and 7 eV, respectively. For Cs, according to these calculations, d bands lie too low in energy and f bands too high to account for the observed absorption peak at 5 eV. Except for Cs then, present calculations indicate that, insofar as energy separation is concerned, transitions to d- or f-like states could account for the observed high-energy peaks.

We do not believe, however, that such transitions can be responsible for the observed absorption. In Cs, where the absorption is strongest, the observed peak falls at the wrong energy. In all of the materials, it is very difficult to understand the large relative magnitude of the high-energy peak as compared with the interband peak for the same material. It seems probable that transition probabilities between s-like conduction-band states and excited states above the first band of p symmetry are far too weak to account for such strong absorption. It would be most useful to have this point confirmed by realistic calculations of the absorption expected from transitions to higher bands. Present calculations of interband absorption are based on a single pseudopotential model that includes only excitation to the first excited band.[24,25]

We have considered two types of collective effects that might contribute to optical absorption above the plasma frequency. The first is due to Hopfield.[26] He shows that the screening of the lattice vibrations by the electron sea becomes less effective at frequencies just above the plasma frequency, so that the free-carrier absorption is enhanced in this region. We have argued in our previous papers that this effect is too small and gives a peak at too low energies in σ to account for our observations.

A second possible explanation of our data involves an absorption process which produces a final state consisting of a plasmon plus an electron-hole pair. Lundqvist has predicted the existence of such a process on the basis of a rather elaborate many-body theory.[27] According to Lundqvist, the high-energy absorption has a threshold at the plasmon energy plus the interband threshold and has a maximum at somewhat higher energy.[28] The position of this peak depends on the details of the calculation but can be estimated approximately from the separation between the quasiparticle peak and plasmon satellite peak occurring in the spectral weight function of his theory. This satellite structure is separated by $1.5\hbar\omega_p$ from the quasiparticle peak and thus should produce a peak about $1.5\hbar\omega_p$ above the interband peak in $\sigma(\omega)$. As noted above in item (iv), our peak positions agree quite well with this prediction. Lundqvist's theory also predicts that the absorption strength should increase with atomic number for the alkali metals; such a trend is found in our data.

The relative magnitude of our observed peaks is not in good agreement with Lundqvist's predictions. For Na, Lundqvist and Lydén calculated a magnitude for absorption due to such plasmon-assisted transitions that is approximately 50% of that due to direct transitions.[27] The ratio of the magnitude of the high-energy peak to the interband peak should be comparable for all of the alkali metals since the same transition matrix elements in $\sigma(\omega)$ control the strength of both the interband transitions and the plasmon-assisted transitions. The ratio should probably increase slightly for the heavier alkali metals whose less dense electron gases couple more strongly to the quasiparticle states in this theory. As noted in item (iii) of the summary above, the ratio of high-energy to interband peaks ranges from 0.5 to 2.5 with no obvious trends visible as atomic number is increased. Thus the observed magnitudes are clearly larger than those expected theoretically.

The discrepancy may be much worse than Lundqvist's theory would suggest, since the theory includes interaction effects only to the lowest order in the coupling between an electron (or hole) and the density fluctuations. Hermanson carries the calculation to higher order and finds that the strength of the plasmon replica is reduced to about 5% of the quasiparticle peak.[29]

In their present form, neither one-electron nor many-body theories can adequately account for the large absorption observed above the plasma energy in the alkali metals. Since the many-body calculations are quite complicated in execution, it seems likely that a final theoretical explanation will require more realistic calculations within the framework of many-body theory.

†Research sponsored by the U. S. Atomic Energy Commission under contract with Union Carbide Corp. and by N. S. F. Grant No. GP11917.

*Research Assistant, University of Tennessee, Knoxville, Tenn. Present address: Phys. Dept., University of Wisconsin, Madison, Wisc. 53706.

‡Consultant, Oak Ridge National Laboratory, Oak Ridge, Tenn. 37830.

[1]U. S. Whang, E. T. Arakawa, and T. A. Callcott, Phys. Rev. Letters 25, 646 (1970).

[2]U. S. Whang, E. T. Arakawa, and T. A. Callcott, J. Opt. Soc. Am. 61, 740 (1971).

[3]U. S. Whang, E. T. Arakawa, and T. A. Callcott, Phys. Rev. B 5, 2118 (1972).

[4]J. C. Sutherland and E. T. Arakawa, J. Opt. Soc. Am. 57, 645 (1967); 58, 1080 (1968); J. C. Sutherland, R. N. Hamm, and E. T. Arakawa, *ibid.* 59, 1581 (1969).

[5]H. Mayer and B. Hietel, in *Optical Properties and Electronic Structure of Metals and Alloys*, edited by F. Abeles (North-Holland, Amsterdam, 1966).

[6]N. V. Smith, Phys. Rev. 183, 634 (1969); Phys. Rev. B 2, 2840 (1970).

[7]M. H. Cohen, Phil. Mag. 3, 762 (1958).

[8]R. N. Hamm, R. A. MacRae, and E. T. Arakawa, J. Opt. Soc. Am. 55, 1460 (1965).

[9]W. R. Hunter, J. Opt. Soc. Am. 54, 15 (1964); 55, 1197 (1965).

[10]U. S. Whang, E. T. Arakawa, and R. N. Hamm (unpublished).

[11]S. Yamaguchi and T. Hanyu, J. Phys. Soc. Japan 31, 1431 (1971).

[12]R. E. Palmer and S. E. Schnatterly, Phys. Rev. B 4, 2329 (1971).

[13]H. E. Ives and H. B. Briggs, J. Opt. Soc. Am. 26, 238 (1936); 26, 247 (1936); 27, 181 (1937); 27, 395 (1937).

[14]H. Mayer and M. H. El Naby, Z. Physik 174, 280 (1963).

[15]R. Althoff and J. H. Hertz, Infrared Phys. 7, 11 (1967).

[16]J. H. Hodgson, Phys. Letters 7, 300 (1963).

[17]C. Kunz, Z. Physik 196, 311 (1966).

[18]J. L. Robin and P. E. Best, Proc. Phys. Soc. (London) 79, 110 (1962).

[19]J. B. Swan, Phys. Rev. 135, A1467 (1964).

[20]T. Kurosawa, in *Dynamical Processes in Solid State Optics*, edited by R. Kubo and H. Kamimura (Benjamin, New York, 1967).

[21]R. G. Oswald and T. A. Callcott, Phys. Rev. B 4, 4122 (1971).

[22]J. F. Kenney, Quarterly Progress Reports of Solid State and Molecular Physics Group, MIT Report No. 53, 1964 (unpublished); MIT Report No. 66, 1967 (unpublished).

[23]F. S. Ham, Phys. Rev. 128, 82 (1962); 128, 2524 (1962).

[24]P. N. Butcher, Proc. Phys. Soc. (London) A64, 7650 (1951).

[25]A. O. E. Animalu, Phys. Rev. 163, 557 (1967); Phys. Rev. B 2, 282 (1970).

[26]J. J. Hopfield, Phys. Rev. 139, A419 (1965).

[27]B. I. Lundqvist, Ph. D. thesis (Chalmers Tekniska Högskola, Göteberg, Sweden, 1969) (unpublished).

[28]B. I. Lundqvist and C. Lydén, in *Proceedings of the Electronic Density of States Symposium* (U. S. GPO, Washington, D. C., 1969), p. 50.

[29]J. Hermanson, Solid State Commun. 9, 1075 (1971); Phys. Rev. B 6, 400 (1972).